

## Ablation mechanism of TaC coating fabricated by chemical vapor deposition on carbon-carbon composites

LI Guo-dong(李国栋)<sup>1,2</sup>, XIONG Xiang(熊翔)<sup>1</sup>, HUANG Ke-long(黄可龙)<sup>2</sup>

1. State Key Laboratory of Powder Metallurgy, Central South University, Changsha 410083, China;

2. School of Chemistry and Chemical Engineering, Central South University, Changsha 410083, China

Received 10 August 2009; accepted 15 September 2009

**Abstract:** Ablation characteristics and mechanism at high temperature for TaC coatings on carbon-carbon composites were investigated by ablation experiments with low power laser and oxyacetylene flame. The results show that the TaC coating is decomposed at the initial stage of laser ablation in atmosphere, and free carbon diffused to the surface, then oxidized to the melt including carbon, oxygen and tantalum. With the increase of ablation time, the melt is oxidized to low valent tantalum-oxide and Ta<sub>2</sub>O<sub>5</sub> is formed finally. During the melt cooling, needle-like crystals of Ta<sub>2</sub>O<sub>5</sub> are precipitated. Between the melt and TaC coating, there exists a diffusion transition layer with thickness of 1–2 μm. The transition layer consists of fine crystals and pores including carbon, oxygen and tantalum. The oxyacetylene flame ablation at 2 300 °C results in the rapid oxidation of TaC and formation of protective liquid films of tantalum oxide on the coating surface, where the liquid film can fill up the cracks and cover the coating. In such case, the oxidation mechanism of TaC is converted to the oxygen solution and diffusion control mechanism.

**Key words:** TaC coating; oxidation; ablation mechanism; carbon-carbon composites

### 1 Introduction

Carbon-carbon(C/C) composites are easy to be oxidized and ablated at high temperature and high-speed gas jet with rapid ablation rate exponential to the pressure of combustion chambers, which limits their potential application in new type and high performance aerospace vehicles[1–3]. To prepare coatings on C/C composites with good resistance to high temperature, oxidation, washout and ablation is an important method to promote the performance and application of C/C composites[4–7]. Coatings, such as SiC, Si<sub>3</sub>N<sub>4</sub>, MoSi<sub>2</sub>, borate glass, etc, exhibit good antioxidation, but their oxidation resistant temperatures are below 1 800 °C in general. The inoxidizability mechanism for coatings below 1 700 °C has been investigated by many researchers. LEE and HYEOK[8] found that the ablation property of the obtained SiC coating prepared by SiO<sub>2</sub> deoxidizing carburization is enhanced with increasing the reaction time and synthesized temperature. In addition, the ablation performance of SiC coating is

dependent on coating grain size and the crystal structure and orientation. The SiC coating ablation performance is similar to its inoxidizability below 1 650 °C, while behaves abnormal at 1 800 °C [8]. HUANG[9] and CUI[10] studied the ablation properties of C/C composites containing TaC coating, and found that it shows better ablation resistance than C/C composites.

TaC is one of the materials with higher melting point (3 880–4 000 °C [11]), together with high hardness, good resistance to washout and erosion, and good chemical compatibility with C/C composites. Therefore, the TaC coating is an excellent choice for the C/C nozzle throat of solid rocket motor (SRM)[12–14]. However, there are few reports on the preparation of TaC ablation-resistance coatings and its ablation mechanism in detail. Accordingly, it is of great significance to study the oxidation ablation process and mechanism for TaC coatings at high temperature.

In this work, the TaC coatings were fabricated by chemical vapor deposition (CVD) method and their ablation properties were investigated by low power laser and oxyacetylene flame at 2 300 °C. In addition, the

**Foundation item:** Project(2007AA03Z110) supported by the National Hi-tech Research and Development Program of China; Project(50721003) supported by the National Natural Science Foundation of China; Project(20070420822) supported by China Postdoctoral Science Foundation; Project(2007RS4027) supported by the Postdoctoral Science Foundation of Hunan Province, China; Project(2007) supported by the Postdoctoral Science Foundation of Central South University, China

**Corresponding author:** LI Guo-dong; Tel: +86-731-88830899; E-mail: lgd63@163.com

oxidation process and ablation mechanism for TaC coating in the oxidation atmosphere over 2 000 were discussed.

## 2 Experimental

### 2.1 Sample preparation

The quasi-3D C/C composite with density of  $1.82 \text{ g/cm}^3$  was chosen as the matrix material. The sample size (diameter  $\times$  length) was  $30 \text{ mm} \times 10 \text{ mm}$ , and the ablation plane was parallel to the fiber felts. The TaC coating was prepared in the isothermal chemical vapor deposition furnace by the deposition technique reported in Refs.[14–15]. The coating structure and morphology were characterized by X-ray diffractometer (D/max 2550 VB) using  $\text{Cu-K}\alpha$  radiation and scanning electron microscope (JSM-6360LV) with energy dispersive X-ray spectrometer (EDS).

### 2.2 Ablation equipment and process

The laser ablation equipment is YAG(Nd) pulse laser (wave length  $1.06 \mu\text{m}$ ) with following parameters: frequency 20 Hz, pulse width 1 ms, laser spot diameter 2 mm, monopulse energy 40 J and working voltage 400 V, 440 V. The laser heating ablation was carried out on TaC coatings for 2, 30, and 120 s in atmosphere.

The oxyacetylene flame was adapted from the oxyacetylene torch. The large size torch blowpipe was adopted with the volume ratio of  $\text{O}_2$  to  $\text{C}_2\text{H}_2$  4:1. Before testing, the flame temperature was measured by graphite blocks. After checking the temperature without fluctuation, the flow and height of oxyacetylene flame and the measuring position could be fixed. Then the thermometric graphite block was removed and test samples were placed on the measuring position. The ablation time and temperature were recorded, and after the given time, the test sample was removed rapidly and cooled in air.

## 3 Results and discussion

### 3.1 Structure and morphology of TaC coating

Fig.1 shows the typical XRD pattern of the TaC coatings. It is seen that only the diffraction peaks of TaC peaks can be observed in a sharp profile, which indicates that the TaC coating obtained is pure. The SEM images of TaC coating are shown in Fig.2. Combining the energy spectrum analysis of the coating fracture surface (Fig.2(b)), it can be found that the Ta content is almost homogenous without impurity inside or outside the coating. The thickness of prepared coating is about  $314 \mu\text{m}$ , exhibiting no surface and interlaminar cracks, with loose surface and dense interior layer, and firm combination with the C/C substrate. From the substrate

to surface, the coating can be sequentially divided into the fine-grained dense area ( $< 150 \mu\text{m}$ ), coarse-grained dense area ( $150\text{--}250 \mu\text{m}$ ) and surface loose area ( $250\text{--}341 \mu\text{m}$ ). The TaC structure is uniform in all areas and the three areas have no obvious transition interface.

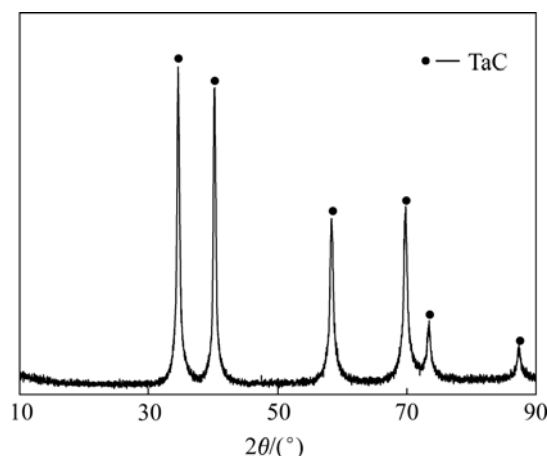


Fig.1 XRD pattern of TaC coating

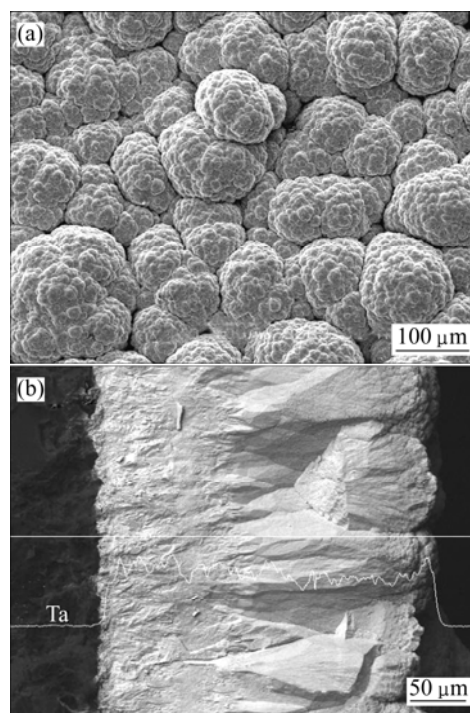
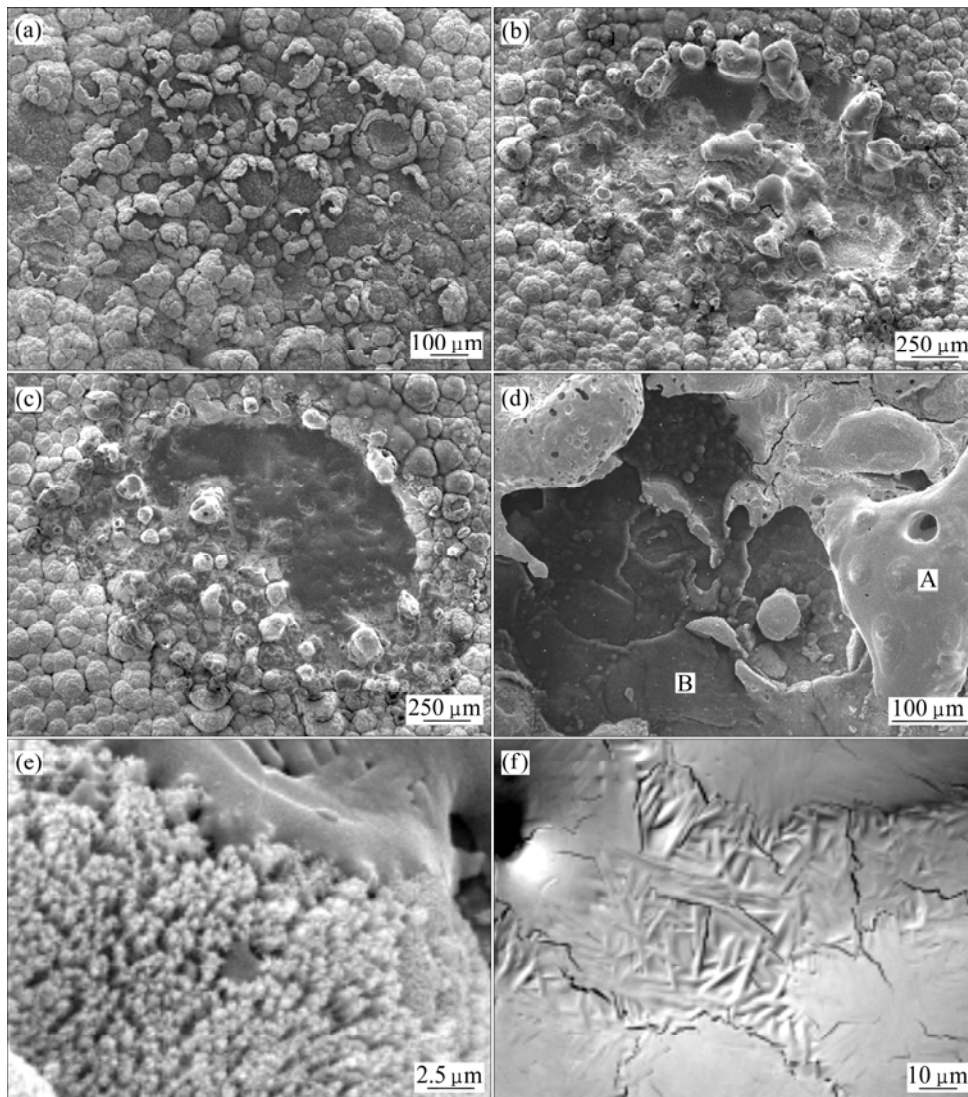


Fig.2 SEM images of TaC coating: (a) Surface morphology; (b) Cross-section morphology

### 3.2 Ablation characteristics of TaC coating by low power laser

Fig.3 shows the surface morphologies of the TaC coating ablated for different time under the working voltage of 400 and 440 V. It can be seen that only local break-up and darkened color can be observed after laser ablation for 2 s (Fig.3(a)); obvious melt appears in small amount with irregular and bubble shape after laser ablation for 30 s (Fig.3(b) and (e)); the melt increases to



**Fig.3** Surface morphologies of TaC coating ablated by low power laser for different time: (a) Ablated for 2 s, 400 V; (b) Ablated for 30 s, 400 V; (c) Ablated for 120 s, 400 V; (d) Ablated for 2 s, 440 V; (e) Edge part of Fig.3(b); (f) Square area of Fig.3(c)

form liquid plane without bubbles after laser ablation for 120 s (Fig.3(c), (f)).

In conventional oxidation for TaC at low temperature ( $< 1500^\circ\text{C}$ ) in air, it is well known that TaC begins to be oxidized into  $\text{Ta}_2\text{O}_3$  over  $500^\circ\text{C}$ , then form  $\text{Ta}_2\text{O}_5$  particles over  $700^\circ\text{C}$  [16]. As far as laser ablation in a short time (2 s) is concerned, the appearance of fracture and break-up on the particle is due to the large expansion coefficient of TaC crystals and local high temperature caused by laser, which leads to the rapid fracture of TaC crystals. The warp deformation of particle shell results from the TaC oxidized to tantalum oxide of low melting point.

Fig.3(e) shows a magnified description of the melt edge of Fig.3(b), where the temperature is a little lower and only a small quantity of melt occurs. There mainly exists white needle-like tantalum oxide aggregation with excellent wetting property to the melt.

Fig.3(f) shows the magnified middle melt region of Fig.3(c). It can be seen that many needle-like crystals precipitated from the melt, which characterizes  $\text{Ta}_2\text{O}_5$  crystals from the melt during cooling. Such precipitates can effectively retard the crack extension for the solidified melt in cooling process.

Fig.4 shows the SEM images of the coating fracture surface after laser ablation for 120 s. Obviously, there is a transition region of  $1\text{--}2\ \mu\text{m}$  (region 2) between the cooled melt (region 1) and TaC coating (region 3). No apparent interface can be seen among the above three regions, and the transition region is composed of pores and fine crystals that were indicated as Ta, O and C by EDS. The occurrence of transition region is beneficial to the wetting and spreading of the surface tantalum oxide melt, and leads to the good bonding property of melt with the TaC coating.

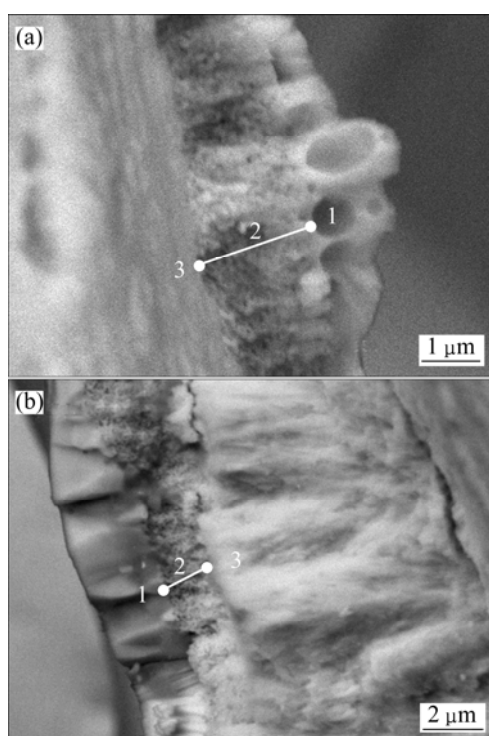


**Fig.4** Fracture SEM images of TaC coating after ablation for 120 s: (a) Fracture surface on the ablative marginal zone; (b) Fracture surface on the ablative center

### 3.3 Ablation process analyses for TaC coating by low power laser

With the increase of laser heating time, the temperature of coating surface rises rapidly up to 2 000 °C. The coating oxidation is accelerated and the tantalum oxide melt occurs soon. After heating for 30 s, large-area melts can be observed (Figs.3(b) and (e)), and further heating results in more and thicker melts (Figs.3(c) and (f)), suggesting the increment of oxide. It is confirmed by EDS that the white melt transforms from the low valent tantalum oxide to  $Ta_2O_5$  gradually with the prolonged heating.

It is noteworthy that the laser heating ablation can not be simply regarded as the heating oxidation process in atmosphere. It can be seen from Fig.3(d) that there is no melt in the region B, indicating the morphology of the coating broken up by laser heating. Region A suggests the melt resulting from the break up of region B and formed by the oxidizing and melting under laser heating. The chemical composition in Fig.3(d) was analyzed by EDS and listed in Table 1. It can be seen that the melt in region A contains oxygen while in other positions (such as region B), the main component is free carbon, together with rare oxygen and small amount of tantalum. This implies that at the initial stage of laser heating, the TaC coating is not mainly oxidized into CO or  $CO_2$ , instead, it

is obviously decomposed. Due to the large relative atomic mass of tantalum, the diffusion of Ta is slow. For the carbon has a small atomic mass, it can diffuse to the surface quickly. With the increase of laser power, the content of free carbon increases and even in the melt region A, considerable amount of free carbon can be obtained. Therefore, the oxidation process at the initial stage of laser ablation is different from that of slow heating. This phenomenon may be explained as follows: on the one hand, when the TaC coating is under the rapid heating of laser, the oxygen content is severely insufficient; on the other hand, the coating is composed of nanoparticles with high interface energy, porosity and specific area, which is easy to be endothermic. Then the local temperature will be excessively high, resulting in the occurrence of decomposition reaction. This is very meaningful to the mechanism analysis of oxidation ablation for the TaC coating applied in the solid rocket with high enthalpy and thermal shock.

The surface melt is thin with many bubbles (Fig.4(a)), resulting from the fact that the TaC coating is not completely covered by the melt and it is rapidly oxidized together with releasing of certain amounts of reaction gas. And the oxidation process is controlled by the reaction mechanism of oxygen and TaC coating. In Fig.4(b), it can be seen that the surface melt is thick without bubbles due to the complete covering of the TaC coating by  $Ta_2O_5$  melt. Thus the coating is not exposed directly to oxygen; resulting in a slow oxidation rate. Besides, the low melt viscosity favors bubbles to be eliminated. Under this circumstance, the oxidation process is controlled by oxygen solution and diffusion mechanism. The oxidation experiment at high temperature has also proved that at 1 000–1 500 °C the oxidation of TaC coating increases rapidly with the increase of temperature, and the coating inoxidizability is rather poor; while over 2 000 °C the oxidation rate of TaC coating decreases obviously and its inoxidizability is largely enhanced. Thus, the melt for resisting oxygen diffusion does not appear on the surface, which is key to determine the oxidation control mechanism and oxidation rate of the TaC coating. The TaC coating covered by tantalum oxide melt will be oxidized or ablated depending on the solution concentration and diffusion velocity of the oxidized gas in the melt. Due to the much smaller amount of oxygen solved in the  $Ta_2O_5$  melt and slower speed of the corresponding oxygen diffusion, as compared with those supplied by rocket combusting gas, the rapid oxidation of the TaC coating can be retarded and the ablation rate can be decreased. From Fig.4, the morphology and thickness of the transition

**Table 1** Chemical composition of TaC coating by EDS

Region	C	Ta	O	$x(\text{C}):x(\text{Ta}):x(\text{O})$
All regions in Fig.2(a)	50.1	49.9	0	1:1:0
All regions in Fig.3(d)	94.0	1.8	4.2	51.6:1:2.3
Region A in Fig.3(d)	36.1	38.6	25.3	1.4:1.5:1
Region B in Fig.3(d)	98.0	2.0	0	49.3:1:0

layer are almost constant. To some extent, the oxidation macrokinetics for the TaC coating can be characterized by the moving rate of the transition layer.

Considering that the  $\text{Ta}_2\text{O}_5$  melt has a large expansion coefficient and its temperature is higher than that of the substrate or the underlying coating, the occurrence of cracks during cooling is inevitable under the large cooling rate and temperature gradient. However, as shown in Fig.3(f), needle-like  $\text{Ta}_2\text{O}_5$  crystals will be precipitated from the melt during slow cooling, which can effectively retard the crack propagation of solidified melt. It is also seen that lots of needle-like crystals appear on the ablative sample surface after ablation in the oxyacetylene flame at 2 300 °C. The XRD results show that such needle-like crystals are tetragonal  $\text{Ta}_2\text{O}_5$  crystals (Fig.5). Then the  $\text{Ta}_2\text{O}_5$  melt during cooling will be strengthened similar to the mechanism of the  $\text{Ta}_2\text{O}_5$  crystal whisker reinforced the  $\text{Ta}_2\text{O}_5$  glass. When the  $\text{Ta}_2\text{O}_5$  melt ruptures, the cracks deflect and increase (Fig.3(f)), thus effectively preventing the cooled melt

from severe break-up during cooling process.

### 3.4 Ablation characteristic and process analysis of TaC coating by oxyacetylene flame

Fig.6 shows the SEM images of the TaC coating after oxyacetylene flame ablation at 2 300 °C for 60 s. Despite of the unevenness, the coating surface exhibits a thin melt with little pores and cracks on the melt surface (Fig.6(a)). XRD results show that the melt is tetragonal  $\text{Ta}_2\text{O}_5$  crystals with some orthorhombic  $\text{Ta}_2\text{O}_5$  crystals, which suggests that the melt has precipitated crystals during cooling. From the natural fracture in Fig.6(b), it can be seen that the coating after ablation can be divided

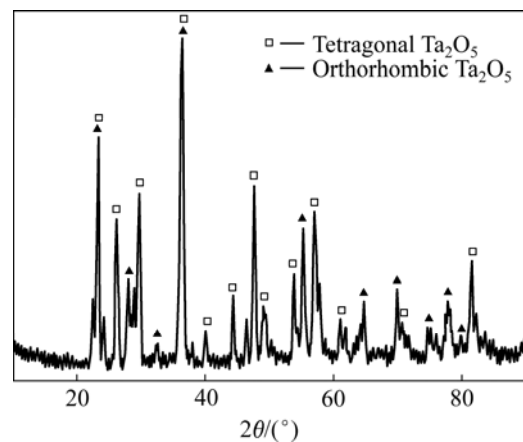


**Fig.5** XRD pattern of TaC coating oxidized by oxyacetylene flame at 2 300 °C for 60 s

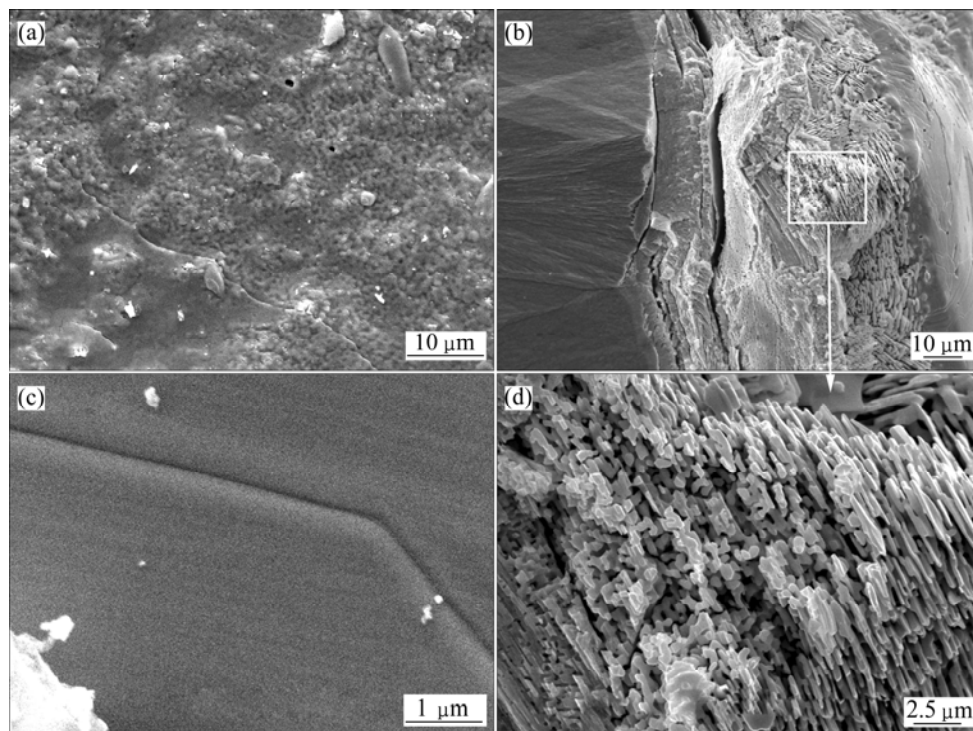


**Fig.6** SEM images of TaC coating after oxyacetylene flame ablation at 2 300 °C for 60 s: (a) Coating surface; (b) Cross-sectional morphology of fracture sample; (c) Local magnified surface morphology; (d) Magnified images from square area of Fig.6(b)

into four parts: the surface is the melt layer starting precipitation of crystals (about 10  $\mu\text{m}$  thickness); next is the porous oxide precipitation layer (about 35–45  $\mu\text{m}$  thickness); the transition layer (about 5–15  $\mu\text{m}$  thickness) and the TaC coating without oxidation, which is closely connected with the transition layer.

The as-fabricated TaC coating exhibits good thermal shock resistance as it has no break-up and large cracks during the whole ablation and cooling process. The cracks shown in Fig.6(b) suggest that there exists stress concentration in regions between the oxide precipitation and transition layer, so does in regions between the transition layer and TaC coating. The laminar cracks are caused by the stress release during the ruptures of the coating.

From the local magnified morphology (Fig.6(d)), the needle-like or columnar crystals can be clearly seen, and their arrays exhibit apparent orientation. The composition in this region is Ta and O with the atomic ratio of 2:(4.5–5) as determined by EDS. By combining with the XRD analysis, the needle-like crystals should be the tetragonal  $\text{Ta}_2\text{O}_5$  crystal, which relates to the morphology of the columnar crystals of the TaC coating. The oxyacetylene flame ablation of the TaC coating is mainly an oxidation process at 2 300 °C. In the beginning stage, the coating temperature is lower than the melting temperature of  $\text{Ta}_2\text{O}_5$ , and the surface coating is loose. When heated by the oxyacetylene flame that is rich in oxygen and flows quickly, the coating will soon be oxidized to form the fine tetragonal  $\text{Ta}_2\text{O}_5$  crystals. Although the oxidation process of TaC is a process of the structure rearrangement, which involves the diffusion reaction of C to the outside and O to the coating interior, the movement of Ta atoms is rather small due to its heavy atomic mass, and the morphology of the TaC columnar crystal is largely inherited. That is why the fine crystal of tetragonal  $\text{Ta}_2\text{O}_5$  grows in a preferred orientation and exhibits the needle-like morphology corresponding to the columnar character of the TaC coating. Some columns are parallel to the coating surface, resulting from the fact that the fine tetragonal  $\text{Ta}_2\text{O}_5$  crystals are partially melt under the burning oxyacetylene flame flow, and the vertical needle-like crystals are toppled by the shear force of the gas flow or surface melt flow.

It can be seen from Fig.6(c) that after the surface generates the  $\text{Ta}_2\text{O}_5$  liquid film and under the action of surface tension, the liquid film can fill in and cap the cracks that exist originally in the surface. Due to the impediment of the  $\text{Ta}_2\text{O}_5$  liquid film, oxidants in the combusting gas will not be in direct touch with TaC, and the further oxidation of TaC will be achieved only by the

solution and diffusion of oxygen through the  $\text{Ta}_2\text{O}_5$  liquid film melt. It follows that the TaC oxidation mechanism is transformed to the oxygen solution and diffusion control type, which agrees well with the results from laser ablation and this is the major reason for the TaC coating with good oxidation and ablation resistance.

## 4 Conclusions

1) The ablation process of the TaC coating by low power laser in air is as follows: the initial thermal shock leads to the local break-up, the decomposition of the TaC coating and the diffusion of free carbon to surface. Then, lots of free carbon are diffused to the surface and oxidized as tantalum oxide melt containing carbon, and the melt is further oxidized to the  $\text{Ta}_2\text{O}_5$  melt gradually. The melt occurrence changes the oxidation mechanism of the TaC coating from the interface reaction control mechanism to the diffusion mechanism in the way that oxygen is solved and diffused speed in the melt. Between the melt and TaC, there exists the diffusion transition layer with thickness of 1–2  $\mu\text{m}$  that consists of fine crystals and pores. The transition layer is mainly composed of carbon, oxygen and tantalum. The occurrence of the transition layer favors the enhancement of the wetting property of the melt and coating and ablation resistance of coating.

2) The oxyacetylene flame ablation of the TaC coating at 2 300 °C for 60 s is mainly an oxidation process during which TaC is rapidly oxidized to needle-like  $\text{Ta}_2\text{O}_5$ . Then  $\text{Ta}_2\text{O}_5$  is melted and the protective liquid film of tantalum oxide is formed on the coating surface, which can fill in and cap the cracks. The further oxidation mechanism of the TaC coating is transformed to the oxygen solution and diffusion control type.

## References

- [1] DONALD L, SCHMIDT, KENNETH E. Unique applications of carbon-carbon composites materials (Part one) [J]. SAMPE Journal, 1999, 35(3): 27–39.
- [2] BACOS M P, DORVAUXJ M, LAVIGNE O. C/C composite oxidation model : Morphological experimental investigation [J]. Carbon, 2000, 38: 77–92.
- [3] LACHAUD J, ASPA Y, VIGNOLES G L. Analytical modeling of the steady state ablation of a 3D C/C composite [J]. International Journal of Heat and Mass Transfer, 2008, 51(9/10): 2614–2627.
- [4] LEE Y J, JOO H J. Ablation characteristics of carbon fiber reinforced carbon (CFRC) composites in the presence of silicon carbide (SiC) coating [J]. Surface and Coatings Technology, 2004, 180/181(1): 286–289.
- [5] LI Xiu-tao, SHI Jing-li, ZHANG Guo-bing, ZHANG Hua, GUO Quan-gui, LIU Lang. Effect of  $\text{ZrB}_2$  on the ablation properties of carbon composites [J]. Materials Letters, 2006, 60(7): 892–896.

- [6] ZOU Wu, ZHANG Kang-zhu, ZHANG Li-tong. Application of ceramic matrix composite to rocket motor [J]. Journal of Solid Rocket Technology, 2000, 23(2): 60–68. (in Chinese)
- [7] STRIFE J R, SHEEHAN J E. Ceramic coatings for carbon-carbon composites [J]. Ceramic Bulletin, 1988, 67(2): 369–374.
- [8] LEE Y J, HYEOK J J. Ablation characteristics of carbon fiber reinforced carbon (CFRC) composites in the presence of silicon carbide (SiC) coating [J]. Surface and Coatings Technology, 2004, 180/181: 286–289.
- [9] HUANG Hai-ming, DU Shan-yi, WU Lin-zhi, WANG Jian-xin. Ablation property for C/C composites [J]. Transaction of Composites, 2001(3): 76–80. (in Chinese)
- [10] CUI Hong, SU Jun-ming, LI Rui-zhen. On improving anti-ablation property of multi-matrix C/C to with refractory metal carbide [J]. Journal of Northwestern Polytechnical University, 2000, 18(4): 669–673. (in Chinese)
- [11] YE Da-lun, HU Jian-hua. Practical manual for inorganic thermodynamics data [M]. Beijing: Metallurgy Industry Press, 2002. (in Chinese)
- [12] BRUNO, THOMA S, ANTHONY C, PAUL Y, SANJAY B, PAUL J, LYNN D, JOSEPH Z. Net mold tantalum carbide rocket nozzle throat: US Patent, 6673449 [P]. 2004–02–06.
- [13] LI Guo-dong, XIONG Xiang, HUANG Bai-yun. Microstructure characteristic and formation mechanism of crackfree TaC coating on C/C composite [J]. Trans Nonferrous Met Soc China, 2005, 15(6): 1206–1213.
- [14] LI Guo-dong, XIONG Xiang, HUANG Bai-yun. Effect of temperature on composition, surface morphology and microstructure of CVD-TaC coating [J]. The Chinese Journal of Nonferrous Metals, 2005, 13(4): 565–571. (in Chinese)
- [15] LI Guo-dong, XIONG Xiang, HUANG Bai-yun, HUANG Ke-long. Structural characteristics and formation mechanisms of crack-free multilayer TaC/SiC coatings on carbon-carbon composites [J]. Trans Nonferrous Met Soc China, 2008, 18(2): 255–261.
- [16] LI Guo-dong, XIONG Xiang, HUANG Bai-yun, ZENG Yu-lin. Oxidized characteristic and oxidized mechanism of TaC coating [J]. The Chinese Journal of Nonferrous Metals, 2007, 17(3): 360–367. (in Chinese)

(Edited by ZHAO Jun)